T. SMOLINSKI[1]*, L. ZHAO[1], M. ROGOWSKI[1], D. WAWSZCZAK[1],
T. OLCZAK[1], M. BRYKALA[1]

SYNTHESIS AND CHARACTERIZATION OF Co-Cs-Nd-Sr- DOPED PEROVSKITE-RUTILE-TYPE STRUCTURE

The perovskite type matrix is considered as solidification material for high-level radioactive waste. In this work the perovskite-rutile-type matrix doped by Co, Cs, Nd and Sr which simulate nuclear waste was prepared by sol-gel route. The material was characterized by several methods such as: X-ray diffraction, energy dispersive X-ray spectrometer, and particle induced X-ray emission combined with Rutherford backscattering spectrometry. The analyzes confirmed chemical composition Co-Cs-Nd-Sr-doped perovskite-rutile-type structure. A virtual model of the pellet`s structure was created non-destructively by Roentgen computed micro-tomography. The leaching tests confirmed high chemical resistance of the matrix.

Keywords: Synroc, X-ray diffraction, Rutherford backscattering, particle-induced X-ray emission, Roentgen computed micro-tomography

1. Introduction

Synthetic Rock (Synroc) was invented in 1978 by Prof. Ringwood of the Australian National University [1,2]. Generally speaking it is advanced ceramic mineral comprising geochemically stable natural titanates which can immobilize different types of radioactive and fissile elements, including uranium and thorium. These elements, present mostly in the ionic form in low- and high-level radioactive wastes, could be incorporated into the crystal or amorphous structures of the synthetic rocks. The main minerals making up Synroc are hollandite ($BaAl_2Ti_6O_{16}$), zirconolite ($CaZrTi_2O_7$) and perovskite ($CaTiO_3$). Different forms of Synroc have been developed to deal with wastes for which no current route is available for disposal. Zirconolite and perovskite are the major host platforms for the long-lived actinides, especially perovskite, which is mainly considered for the immobilization of strontium (Sr) and barium (Ba). Hollandite is principally applied to immobilize cesium (Cs), rubidium (Rb) and barium. Different types of Synroc with unique structures could hold many forms of radioactive ions according to their chemical characters and unique structures. The method of synthesis has been reported in our recent publications in 2014 [3,4]. In the present work, developed at Institute of Nuclear Chemistry and Technology the Complex Sol-Gel Process (CSGP), previously used for synthesis various types' ceramic materials [3-7], was applied to synthesize the perovskite-rutile-type Synroc. To simulate the incorporation process of the high level nuclear waste into a matrix, ionic liquid forms of non-radioactive Co, Cs, Nd and Sr, were used. Surrogates are widely used in the research and development of nuclear waste-forms, providing detailed insight into the chemical and physical behavior of the wasteforms whilst avoiding the widespread (restricted and costly) use of radio-toxic elements in the laboratory [8-10]. The investigated matrix should permanently immobilize the elements. The leaching analyzes were performed to confirm this assumption. Moreover, the structural information on this type of Synroc synthesized by the CSGP has not yet been reported. The structural and chemical analysis of perovskite-rutile-type Synroc was carried out by several instrumental methods. The non-destructive testing of the synthesized material was performed with the use of Roentgen computed micro-tomography technique.

The goal of the series of structural characterization studies is to show that the material synthesized by a sol-gel method can be successfully applied for solidification of elements which are present in nuclear waste (Fig. 1). It could be used also as a ceramic matrix for disposal of radioactive wastes generated by High Temperature Gas Cooled Reactors, such as a generation IV reactors.

[1] INSTITUTE OF NUCLEAR CHEMISTRY AND TECHNOLOGY (INCT), 16 DORODNA STR., 03-195 WARSAW, POLAND

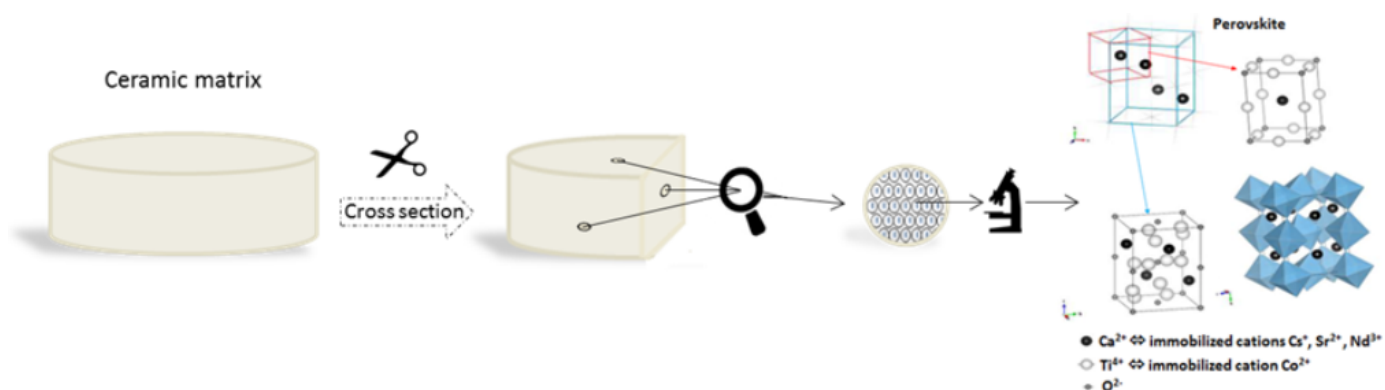* Corresponding author: t.smolinski@ichtj.waw.pl
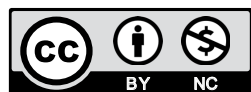
Fig. 1. A diagram of immobilization of the nuclides into perovskite matrix

2. Experimental

2.1. Material

The following reagents were used: titanium (IV) chloride (Sigma Aldrich, 98%), calcium nitrate (Sigma Aldrich, 99%), L-ascorbic acid (VWR, pharmaceutical grade), cesium nitrate (Alfa Aesar, 99.8%), strontium nitrate (Alfa Aesar, 99.8%), cobalt (II) nitrate hexahydrate (Sigma Aldrich, 99%) and neodymium (III) nitrate hexahydrate (Sigma Aldrich, 99%). All other reagents used were of analytical grade.

2.2. Synroc preparation

The method of synthesis of perovskite-type Synroc by the method of a CSGP has been described in our previous publications in details [3,4]. In this work, $TiCl_4$ was dissolved in concentrated HCl to form a 4 M Ti solution. Nitric acid was then added for chloride elimination which is achieved by distillation. $Ca(NO_3)_2$ was added before the addition of 10% M (M = Co, Cs, Nd and Sr – 2.5% of each) surrogates. These elements were chosen to simulate specific radionuclides which are present in high level waste (see Table 1). TiO_2 sol solution prepared as in [7] was added to improve leaching resistance of the material [2]. Designed composition of the material was:

$$Ca_{0.9}(Co, Cs, Nd, Sr)_{0.1}TiO_3 + TiO_2 \qquad (1)$$
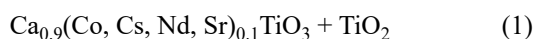
The ratio of the added rutile to perovskite was approx. 0.25. The addition of rutile should increase the chemical resistance of the entire matrix [1,3].

TABLE 1

Surrogate element used and radionuclides represented

Surrogate metal	Radionuclide represented
Cobalt (Co)	^{60}Co
Cesium (Cs)	^{137}Cs
Neodymium (Nd)	^{238}U and others isotopes plus transuranium elements
Strontium (Sr)	^{90}Sr

The whole system was remolded by evaporation from sol to gel form. The final processes were drying, grinding and formation of the pellets by pressing of irregular grains of titanates. Powders were pressed on a hand press in double-sided dies for compacts with a diameter of 20 mm under a pressure of 10 MPa. To increase the strength of the compacts and reduce friction during pressing, 3% polyethylene glycol in alcohol, distillated water or 2% aqueous polyvinyl alcohol solution were added to the powders. The last step of presented work was sintering of the pellets at 1200°C for 2 hours in the air. The heating and cooling rate was not higher than 180°C/h. Preliminary experiments for leaching resistance were done. The pellets were treated by deionized water for 30 days under static conditions at 25°C.

2.3. Analytical methods

X-ray diffraction (XRD)

The structure of the material was investigated by powder X-ray diffraction, using a Siemens D500 diffractometer with Cu-Kα radiation (tube output voltage 38 kV and tube output current 30 mA) and scanning range from $2\theta = 10°$ to $2\theta = 80°$ (step 0.02° and rate 2°/min).

Scanning electron microscopy/energy dispersive spectrometry (SEM-EDS)

Scanning electron microscopy with energy dispersive X-ray spectroscopy (SEM/EDS) is the most common microscopic technique for the morphological analysis of nanoparticles. SEM/EDS measurements were performed on a Zeiss Gemini 1530 Scanning Electron Microscope and an SEM/STEM HITACHI 5500 Microscope. Qualitative and semi-quantitative information of the chemical composition of the matrix were confirmed by EDS analysis.

Rutherford backscattering combined with particle-induced X-ray emission (RBS and PIXE)

In order to determine the elemental composition of the Synroc samples, a combination of RBS and PIXE methods was used. In elastic backscattering spectrometry, ion beams of MeV

energy are used and the energy distribution of backscattered ions is measured. Using well known scattering kinematics and cross section of the interaction, the atomic mass of the elements presented in the sample are identified and depth distribution is calculated [11]. RBS is usually employed for the analysis of heavy elements in a light matrix due to its high sensitivity correlated with high cross section of the interaction. In this particular case, the stoichiometry of heavy elements such as Ti, Sr, Nd, Cs and Co was determined. For the RBS, 4 MeV $^7Li^{3+}$ ions were used with the scattering energy detector positioned at 165° to the beam direction. Analysis of the measured RBS spectra was done SIMNRA software [12].

Roentgen computed micro-tomography (μCT)

Roentgen computed microtomography (μCT) was performed on the XRADIA XCT-400 X-ray microtomograph. The X-ray tube was set to 150 kV and 67 μA. A total of 1200 X-ray images were obtained, within the range of 0 to 180°. Exposure time for each image was 15 s. Micro CT allows visualization of the internal structure of a measured object, and is determined by density differences. The technique combining with software allows for 3D reconstruction of scanned object.

Specific surface area of solids is based on the Brunauer-Emmett-Teller method (BET)

The BET surface area analysis was performed by using Quantachrome Autosorb-1, in thermo stated bath at liquid nitrogen temperature of –196.15°C.

Inductively coupled plasma mass spectrometry (ICP-MS)

The concentration of Cs, Sr, Co and Nd in leachant was chemically analyzed by ICP-MS instrument (ELAN DRC II PerkinElmerTM) with a cross-flow nebulizer and a Scott double-pass spray chamber and Ni cones was used in the measurements. Standard solutions (1 mg mL^{-1}) used in ICP-MS analyses were supplied by PerkinElmer.

3. Results and discussion

Obtained ceramic powder was analyzed by XRD. The results are shown in Fig. 2. They reveal one major structure: $CaTiO_3$ with TiO_2 formed during the sol-gel process. Three undefined peaks are presented on the spectra at 25°, 57°, and 66°. According to software data these peaks may origin from: 25° cesium titanium oxide – $Cs_{0.6}Ti_{1.84}O_4$ (orthorhombic – Immm), 57° calcium neodymium titanium oxide – $(Ca_{0.584}Nd_{0.249})$ (TiO_3) (orthorhombic – Pnma), 66° cesium titanium oxide – $Cs_{1.36}(Ti_{1.36}Ti_{6.64})O_{16}$ (tetragonal – I4/m) or calcium titanium oxide – $Ca_4Ti_3O_{10}$ (orthorhombic – Pcab). It is possible that obtained multicomponent material is not a pure phase. Other possible explanation of these phenomena is deformation of the crystal structure because of substitution of the surrogates. This issue needs future investigation. However, the main structure
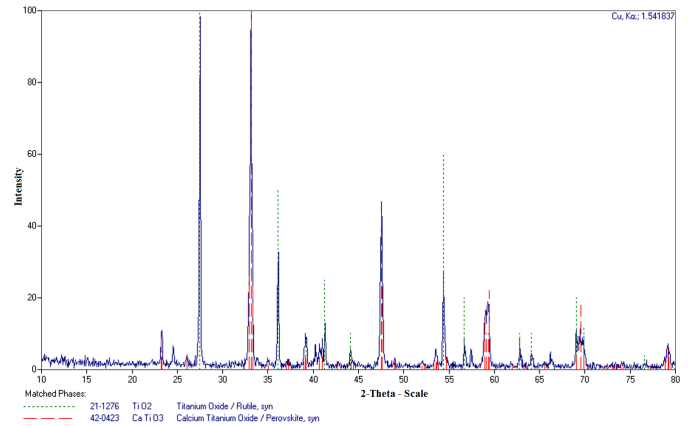

Fig. 2. X-ray diffraction spectrum for the perovskite-rutile-type Synroc $CaTiO_3$ with doping of selected surrogate

is perovskite, whose general formula is ABO_3, consists of an octahedral network with interstitial spaces filled with cations. A three-dimensional network of corner-sharing BO_6 octahedral forms dodecahedral interstices which are large enough to accommodate the A cations [3]. In perovskite, large quantities of radionuclides, such as actinides and rare-earth elements, replace the cation A, while the smaller radionuclides replace the smaller cation B. In the case of $CaTiO_3$, the radionuclide ions such as Cs^+, Sr^{2+} and Nd^{3+} replace the larger cation Ca^{2+}, while the smaller radionuclide ions, such as Co^{2+}, replace the cation Ti^{4+}. The volume of the unit cell was estimated by the Rietveld method. The refinement was carried out with GSAS software, assuming Pbnm space group for an orthorhombic distorted perovskite-type structure. The peaks profiles were studied with the pseudo-Voigt function, that is defined as a linear combination of a Lorentzian and a Gaussian function. The volume of the unit cell increases with increasing the size of the substituting elements (Fig. 3).
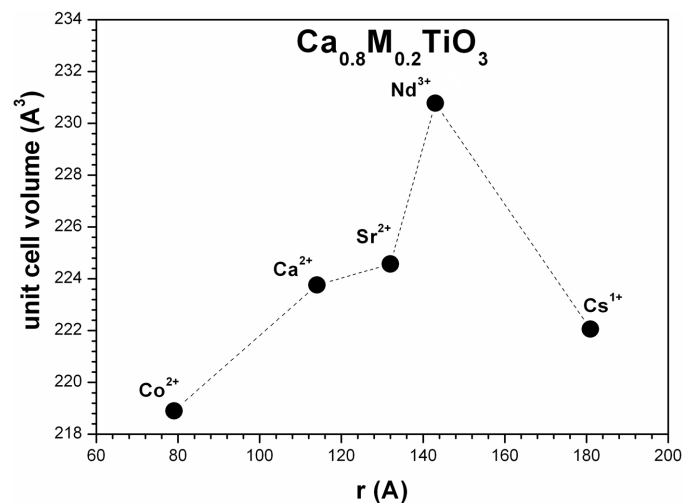

Fig. 3. Dependence of the unit cell volume on the ion radius of substituting element

Even if cesium has the highest ion radius, the insertion of Cs into the $CaTiO_3$ perovskite structure promotes the unit
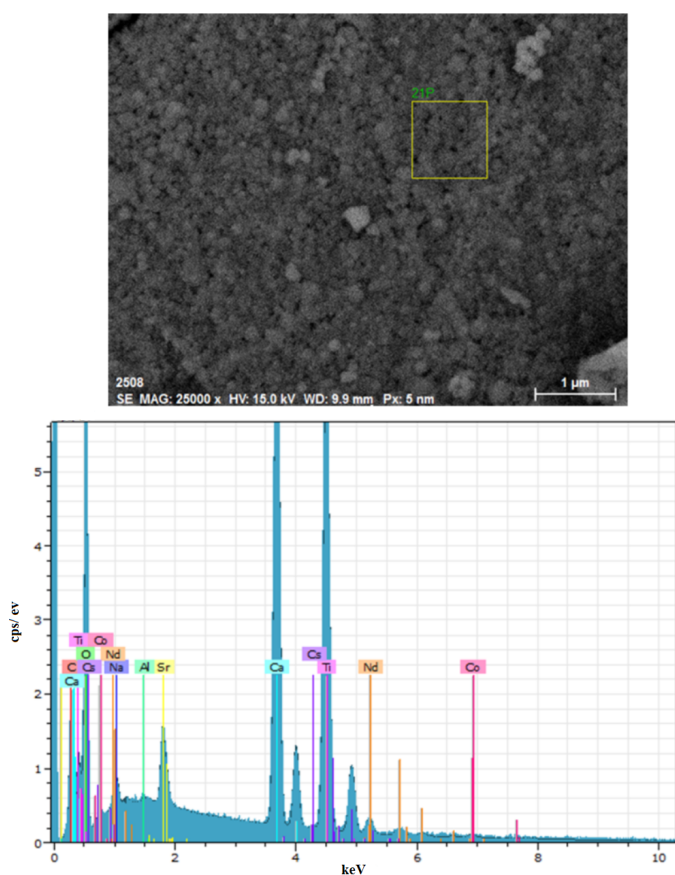
Fig. 4. SEM image of the perovskite-rutile-type Synroc CaTiO$_3$ and energy dispersive spectrometry of the surface element composition of perovskite-rutile-type Synroc CaTiO$_3$

In Fig. 4 the surface image of representative sample is determined by scanning electron microscopy. The EDS spectrum was obtained to determine the elemental composition of that area. The existence of peaks of cobalt, cesium, neodymium and strontium demonstrate that added trace amounts of those ions had been present into the synthesized rock. The signal peak for carbon arises from graphite applied in the sample preparation. Due to the thermal treatment at 1200°C in the alumina crucible, a trace amount of aluminum diffuses into the synthesized rock sample, as shown in the representative EDS spectrum in Fig. 4. Several samples were investigated by EDS analyzes. The average elemental composition on the material is listed in Table 3. Although results are semi-quantitative (analyzes were made from powder material) it confirms presence of all elements used for synthesis especially presence of surrogates into powder grains. For obtaining more specific composition a RBS-PIXE data analyses were performed.

Particle-induced X-ray emission is based on the ejection of inner-shell electrons from the atom and measurement of the subsequently emitted X-rays. Atom identification is according to the energy of the emitted X-rays (Kα, Kβ, Lα, Lβ, Lγ, Mα...) and the concentration of the element is directly proportional to the intensity of the spectral line [1,3]. Due to the high dynamic range of PIXE [14], X-ray energy lines of Sr, Cs, Co and Nd are very well separated. Calculated mass concentration is converted in elemental composition, which was then used as input parameters for the analysis of the RBS spectra. PIXE measurements were performed using a 2 MeV ^{1}H$^+$ beam with two X-ray energy detectors for the detection of low- and high-Z elements. PIXE spectra were analyzed using GUPIX software [15]. Since the sample had a powder structure, they were pressed into pellets, and only the average elemental composition was determined.

cell contraction because of the formation of vacancy in oxygen sites in agreement with the neutrality conditions. The results are shown in Table 2.

TABLE 2

Unit cell parameters estimated by the Rietveld method

T(°C)	Composition	Phase	Size(nm)	a(A)	b(A)	c(A)	V(A^3)
1200	CaTiO$_3$	perovskite	38.00	5.391	5.431	7.642	223.632
1200	CaTiO$_3$ with Nd	perovskite	30.44	5.352	5.533	7.793	230.777
1200	CaTiO$_3$ with Cs	perovskite	22.11	5.368	5.428	7.620	222.059
1200	CaTiO$_3$ with Co	perovskite	28.31	5.373	5.349	7.616	218.901
1200	CaTiO$_3$ with Sr	perovskite	18.88	5.416	5.457	7.598	224.570

TABLE 3

Concentration of each element in the matrix by EDS method

Element	Concentration (wt %)	Error (wt %)
Oxygen	42.02	17.87
Calcium	18.18	2.14
Titanium	34.02	2.90
Cobalt	1.01	0.53
Strontium	1.33	0.55
Neodymium	2.55	0.65
Aluminum	0.06	0.09
Cesium	1.43	0.59
Carbon	2.70	1.72

Due to the limited range of the incidence of Li ions, only the first approximately 1 μm of the sample pellet is analyzed.

The spectral line in light blue in Fig. 5 is a result of computer simulation using SIMNRA software combined with the PIXE results for the Synroc sample. The spectrum for each individual element is also illustrated in different colors. The red dotted line is the experimental result acquired by the data acquisition system. From the spectrum obtained, it can be seen that the simulated and experimental results show a similar trend. The simulation result below the 250 channel, which deviates from the experimental result, is due to energy straggling and double scattering effects of the incidence and backscattered ions that cannot be well simu-
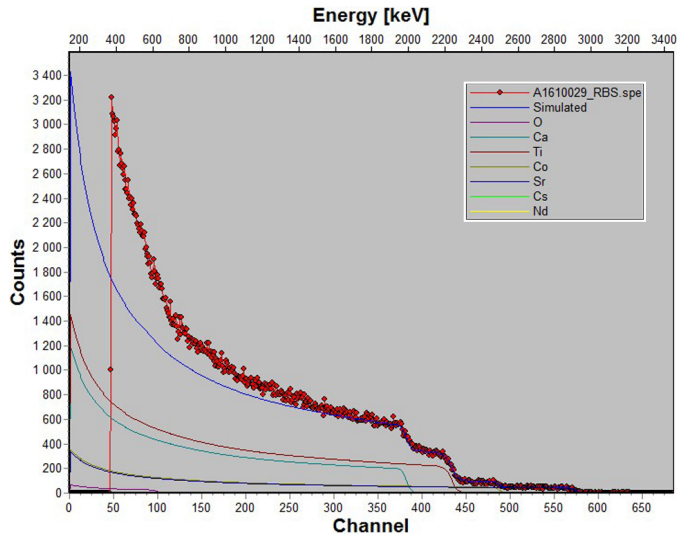
Fig. 5. SIMNRA simulation of EBS spectrum

Fig. 6. Three orthogonal cross-sections of the sample: (A) section, (B) longitudinal and (C) sagittal, and (D) their spatial representation

lated [12-14]. The RBS analysis combined with PIXE confirms that the as-synthesized rock is composed of oxygen, calcium, titanium, cobalt, strontium, cesium and neodymium. The average composition is given in Table 4. Information about the carbon composition is not provided because the signal (energy of the backscattered Li ions from carbon atoms) is below the energy threshold of the ADC set in the measurement (~50 channels) even if carbon exists in the Synroc sample.

TABLE 4

Average element concentration into the matrix by RBS-PIXE

Element	Concentration (Atom %)	Error (Atom %)
Oxygen	61.01	3.24
Calcium	13.86	1.01
Titanium	23.74	1.74
Cobalt	0.36	0.03
Cesium	0.41	0.03
Strontium	0.37	0.03
Neodymium	0.35	0.02

According to this results assuming ratio between doped perovskite and rutile = 0.25 (as it was added during synthesis) the chemical composition of obtained materials is

$$Ca_{0.721} Co_{0.018} Cs_{0.021}Nd_{0.018}Sr_{0.019}TiO_{2.800} + TiO_2 \quad (2)$$

Obtained composition corresponds with designed composition of the ceramic matrix.

Before leaching tests the specific surface area and porosity had been determined. The specific area was measured by BET method in nitrogen. The specific area was 0.01812 m^2/g.

The porosity was determined as a function of sample height using μCT scan. This was done by calculating the porosity of each of the reconstructed sections spaced by the pixel size (16.85 μm) presented in Fig. 6 and Fig. 7. Analysis of porosity as a function of the sample height (Fig. 8) shows that there are no pores, but many cracks. The largest number is in the middle
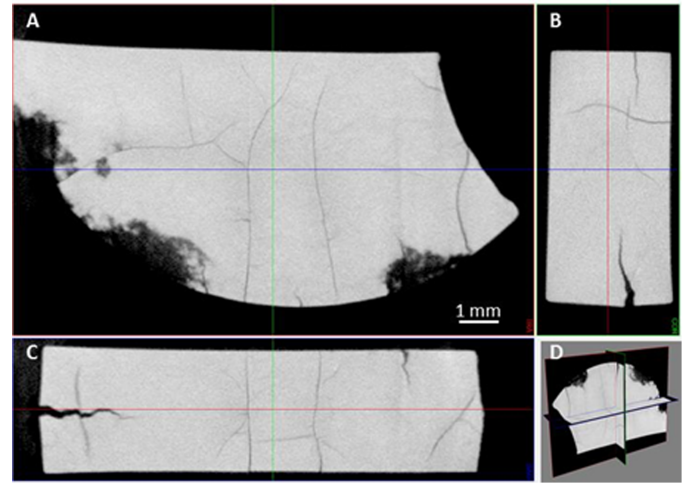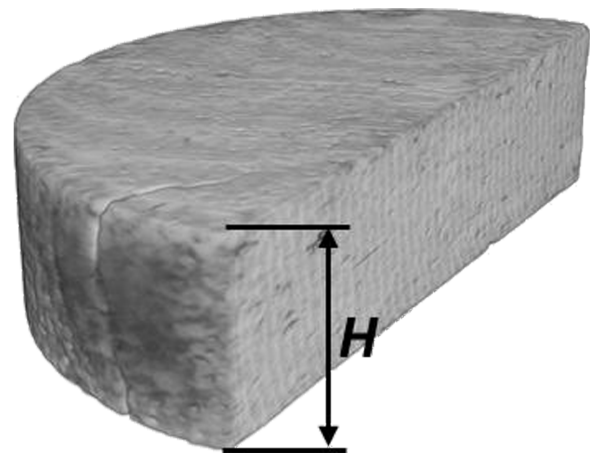

Fig. 7. Three-dimensional reconstruction of the sintered sample to visualize the analysis of porosity as a function of sample height (H)

of the sample. Cracks are the result of sample preparation for tomographic analysis. The pellet cracks during the cutting of the sintered ceramic to the appropriate size.
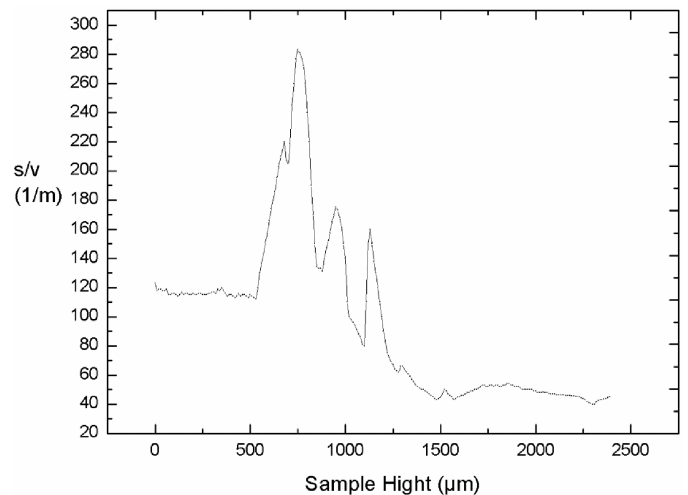

Fig. 8. The specific surface area of cracks per unit volume as a function of sample height

A summary of the porosity analysis in three dimensions and the density of the grid of cracks are shown in Table 5. The density of cracks for the tested sample, expressed as the surface area of cracks per unit volume of the analyzed sample (S/V) amounts to 87.45 (1 / m). Grid cracks are 'open'-cracks that connect to each other and to the surface (98% of all the identified cracks).

TABLE 5

Summary of results of the μCT analysis

Quantitative Parameter	The tested Synroc
Absolute Porosity(%)/Surface Specific Cracks (1/m)	1.44 ±1.2/87.45 ± 9.35
Effective Porosity(%)/Outgoing Surface Cracks (1/m)	1.43 ± 1.2/58.80 ± 7.67
Ineffective Porosity(%)/Internal Cracks (1/m)	0.01 ± 0.1/28.65 ± 5.35

The measured sample had a homogeneous density distribution through the whole volume, as has been shown by the reconstructed images from the analysis of micro-CT (Fig. 7), and very limited porosity. This confirmed the uniform density of the sample produced by the pressing process and should result good leaching resistance.

The leaching resistance of the material was investigated. To compare the leaching of the different cations, it is useful to introduce the leached fraction NL(i), which is obtained by dividing the dissolved mass of the element 'i' (i = Cs, Sr, Co and Nd) by the initial mass of this element in the ceramic matrix. The leaching rate was calculated using equation 3.

$$NL(i) = C_i/(SA/V) \cdot f_i \cdot t \qquad (3)$$

In this expression, C_i is the measured concentration, V the leaching solution volume, f_i the weight fraction of the element 'i' in the matrix as given by the elemental analysis, and SA the specific surface area of the matrix in the experiment. With this definition, the NL(i) values should be the same for the different matrix components in case of congruent dissolution. The results are shown in Fig. 9.

The leaching rates for all immobilized elements were similar. Only Cs leaching rate is a little bit higher. The Cs is a monovalent cation so it is easy for leaching and harder to immobilization into host matrix. For this kind of elements there is specially designed Synroc e.g. hollandite [16]. The lowest and the most constant leaching rate was observed for Co, which leachability is low in general [17]. The leaching resistance is circa around 10^{-8} g/cm^2/day what corresponds with literature values [18].

4. Conclusions

The combination of X-ray diffraction, scanning electron microscopy/energy dispersive spectrometry, Rutherford backscattering and particle-induced X-ray emission techniques have given qualitative and semi-quantitative chemical composition and structural information on obtained matrix, which might be used for the immobilization of radioactive ions from liquid-phase nuclear waste. The XRD technology determined the crystal structure. Two main phases were perovskite CaTiO$_3$ mixed with rutile TiO$_2$ in ratio 3:1. SEM/EDS technology employed for elemental analysis gave information about chemical composition of the material. The obtained perovskite-rutile-type Synroc material was composed of oxygen, calcium, titanium, cobalt, cesium, neodymium and strontium. The detailed composition information was also given by the application of RBS-PIXE. Calculated stoichiometry of obtained matrix is: Ca$_{0.721}$ Co$_{0.018}$Cs$_{0.021}$Nd$_{0.018}$Sr$_{0.019}$TiO$_{2.800}$ + TiO$_2$. The specific surface area was very low c.a. 0.018 m^2/g. The Roentgen computed micro-tomography test reconstructed the image of the Synroc material under X-ray. The analyses fully confirmed
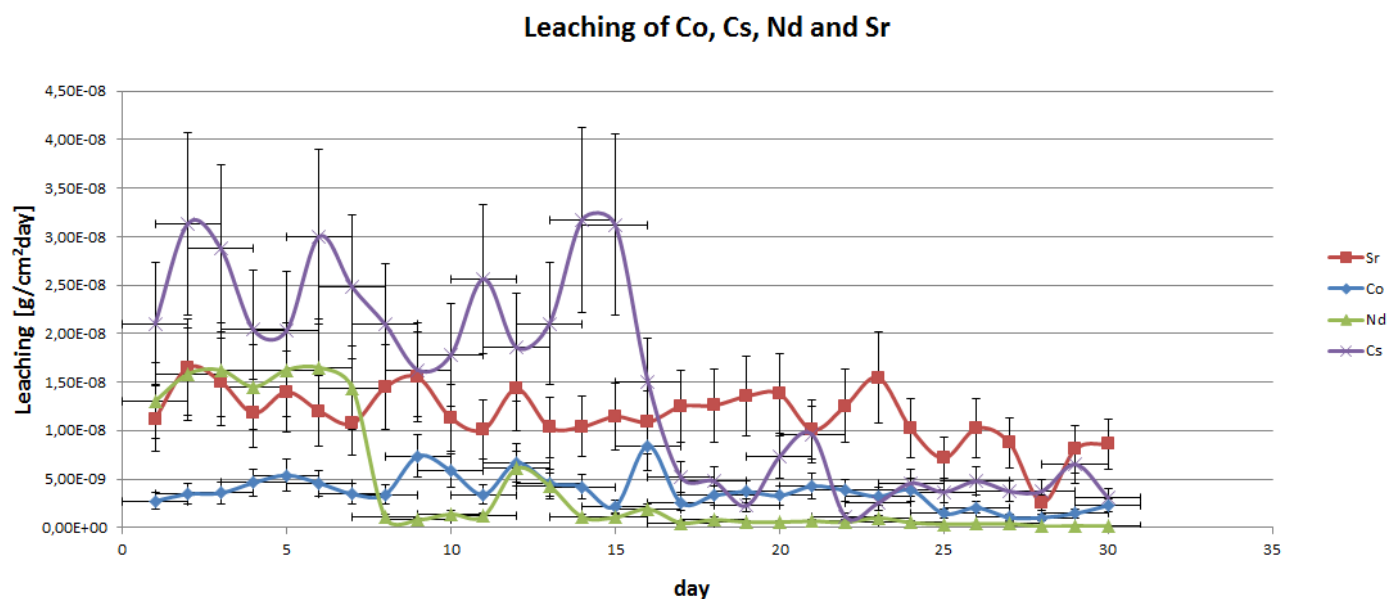

Fig. 9. Resistance of the matrix for leaching of surrogate

the homogeneous density and porosity distribution through the whole volume. These parameters resulted high leaching resistance of the matrix. Average leaching resistance was on the level 10^{-8} g/cm^2/day. This result corresponds with literature parameters. The work is a demonstration of the possible application of the tested methodology for radioactive waste solidification.

REFERENCES

[1] A.E. Ringwood, Am. Sci. **70** (2), 201-207 (1982).

[2] A.E. Ringwood, S.E. Kesson, "Synroc"; in Radioactive Waste Forms for the Future, edited by W. Lutze et R. Ewing, North Holland Physics Publishing (1988).

[3] T. Smoliński, A. Deptuła, T. Olczak, W. Łada, M. Brykała, P. Wojtowicz, D. Wawszczak, M. Rogowski, F. Zaza, J. Radioanal. Nucl. Chem. **299**, 675-680 (2014), DOI:10.1007/s10967-013-2835-x

[4] T. Smolinski, A. Deptula, W. Lada, T. Olczak, A.G. Chmielewski, F. Zaza, Nuclear waste immobilization into structure of zirconolite by Complex Sol Gel Process MRS Proceedings Mater. Res. Soc. Symp. Proc. **1683**, DOI: 10.1557/opl.2014

[5] A. Deptula, W. Lada, T. Olczak, B. Sartowska, A. Ciancia, L. Giorgi, A. Di Bartolomeo, Mat. Res. Soc. Symp. Proc. **498**, 237-242 (1997), DOI: 10.1557/PROC-496-237

[6] M. Brykala, M. Rogowski, T. Olczak, Nukleonika **60** (4), 921-925 (2015), DOI:10.1515/nuka-2015-0122

[7] A. Deptula, M. Brykala, W. Lada, T. Olczak, B. Sartowska, A.G. Chmielewski, Fusion Eng. Des. **84**, 681-684 (2009), DOI:10.1016/j.fusengdes.2008.12.077

[8] Y. Hee-Chul, L. Jae-Hee, K. Jung-Guk, Y. Jae-Hyung, K. Joo-Hyung, JoNET. **34**, (2002).

[9] V.I. Malkovsky, S.V. Yudintsev, E.V. Aleksandrova, Radiochemistry **60**, 648-656 (2018), DOI:10.1134/S1066362218060140

[10] Ch.Z. Liao, Ch. Liu, M. Su, K. Inorg. Chem. **56** (16), 9913-9921 (2017), DOI:10.1021/acs.inorgchem.7b01425

[11] W.K. Chu, J.W. Mayer, Backscattering Spectrometry. Academic Press (1978).

[12] M. Mayer, Technical Report IPP 9/113. Max Planck Institute for Plasma, Germany, (1997).

[13] Y. Wang, M. Nastasi, Handbook of Modern Ion Beam Materials Analysis. Second Edition, Warrendale (2010).

[14] C.G. Ryan, W.L. Griffin, Nucl. Instrum. Methods Phys. Res. Section B, **181** (1-4), 578-585, (2001), DOI:10.1016/S0168-583X(01)00356-1

[15] J.A. Maxwell, J.L. Campbell, Nucl. Instrum. Methods Phys. Res. Section B, **95** (3), 407-421, (1995), DOI:10.1016/0168-583X(94)00540-0

[16] V. Luca, E. Drabarek, C. Griffith, H. Chronis, J. Foy, The Immobilization of Cesium and Strontium in Ceramic Materials Derived from Tungstate Sorbents. MRS Proceedings, 807, 303. (2003). DOI:10.1557/PROC-807-303.

[17] C.W. Kim, J.K. Park, T.W. Hwang, J. Nucl. Sci. Tech. **48** (7), 1108-1114, (2011), DOI:10.1080/18811248.2011.9711796

[18] M.I. Ojovan, W.E. Lee, An introduction to nuclear waste immobilization, Elsevier (2014).